10.1109/ULTSYM.2009.0253

Heterodyne Laser-Doppler Interferometric Characterization of Contour-mode Resonators above 1 GHz

Hengky Chandrahalim
and Sunil A. Bhave
School of Electrical and
Computer Engineering
Cornell University
Ithaca, New York 14853, USA

Ronald G. Polcawich
and Jeff Pulskamp
US Army Research Laboratory
Adelphi, MD 20783, USA

Babak Pourat,
Sebastian Boedecker,
and Christian Rembe
Polytec GmbH
Waldbronn, 76337, Germany

***Abstract*—This paper reports the design and optical characterization of PZT transduced high-overtone width-extensional mode resonators with resonance frequency above 1 GHz. For the first time, a novel technique to measure resonance frequencies and vibrations of contour-mode resonators optically up to 1.2 GHz using only a 618 MHz carrier frequency is demonstrated. The output signal from the photo detector of the vibrometer is digitized by a fast digital oscilloscope and demodulated off-line in a computer. A signal processing algorithm has been developed to acquire frequency components from the photo detector which are higher than the carrier frequency to construct I and Q (in-phase and quadrature) signals from a virtual carrier signal with frequency 2x of the original carrier frequency. This method enabled us to realize an algorithm to extend the measurement bandwidth by a factor of 2 for small vibration amplitudes (< 20 nm).**

I. Introduction

RF MEMS devices such as resonators and filters are normally characterized electrically by using instruments such as network analyzer or spectrum analyzer. These instruments measure resonance frequency (f), insertion loss (IL), and quality factors (Q) of the MEMS resonators and filters. We have demonstrated for the first time a monolithically integrated PZT transduced RF switches and contour mode MEMS filters as a switchable filter array [1]. Due to manufacturing imperfections such as misaligned electrodes, imperfect anchors and sidewall slopes caused by etching, a few of our contour-mode filters exhibit undetermined spurious frequency response. Electrical measurements using network analyzer or spectrum analyzer have limited capability to identify the undesired parasitic modes of vibrations of MEMS resonators and filters that may be introduced due to fabrication errors. These parasitic modes are impossible to mimic in finite element analysis software packages. Therefore, we need another method of looking at these modes to get visual understandings of their existence.

Several research groups have utilized a method based on dynamic force microscopy to characterize subnanometer-scale mechanical vibrations in resonant micro- and nanoelectromechanical systems [2]. By using this method, vibrating structures up to GHz frequency can be characterized. However, this technique requires the AFM tip to make a continuous contact with the surface of the device during characterization. This may cause undesired surface damage or performance drift of the device. Optical measurement facilitates a non-contact characterization technique that circumvents all these problems. Furthermore, it also permits vacuum measurement for resonating RF MEMS devices that are sensitive to air-damping.

Various kinds of optical measurement techniques have been used to characterize MEMS structures. A Stroboscopic interferometer system has been used to measure the in-plane and out-of-plane movements of a microactuator, micromirror array, and microgyroscope [3]. An optical lock-in vibration detection using photorefractive frequency domain processing has been presented [4]. This method is attractive because a narrow bandwidth full-field measurement to characterize amplitude and phase of a vibrating structure can be performed. However, it requires large power laser that continuously impinge the resonator under test. This may cause significant frequency shift during measurement. The homodyne Michelson interferometer stabilized on the quadrature point of the interference signal is a very popular optical measurement technique [5]. These homodyne interferometers can measure amplitudes of mechanical vibrations with sub-nm resolutions and frequencies up to the GHz regime. However, they offer no means of measuring accurate vibration amplitudes of RF MEMS devices because the reference mirror is mounted on a piezoelectric transducer. Rembe $et\ al$ presented a heterodyne interferometer with a well-known frequency response of the detector for vibration frequencies up to 1.2 GHz [6]. This interferometric system has been advanced to a system which has become commercially available as UHF-120 from Polytec. This new interferometer system in combination with a Tektronix frequency generator perform measurement with high accuracy up to 240 MHz [7].

In this paper we demonstrate an improved excitation with the Rohde $\&$ Schwarz generator SMBV100A which makes possible to apply high-power, broad-band excitations with

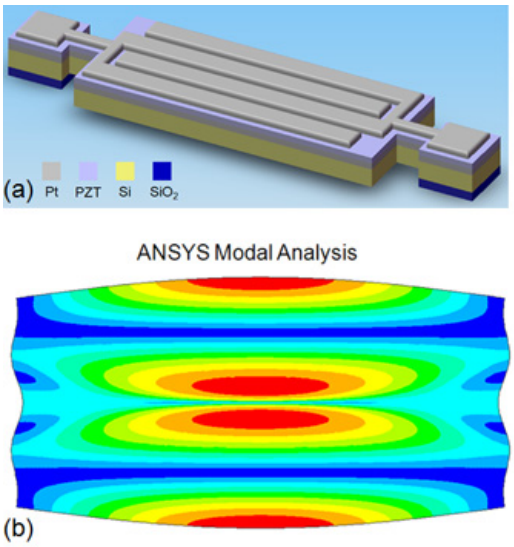

Fig. 1. (a) Schematic of a PZT-on-silicon high-overtone width-extensional mode resonator. (b) ANSYS mode shape of a high-overtone width-extensional mode resonator.

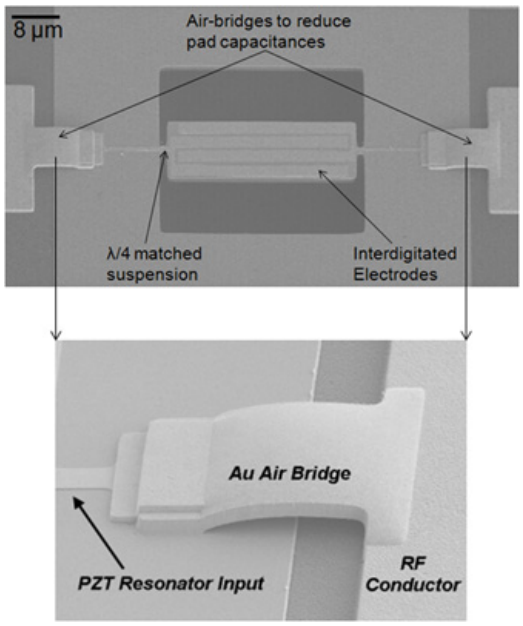

Fig. 2. SEM of the fabricated high-overtone width-extensional mode resonator. The zoom-in picture shows the air-bridge routing that isolates the resonator from the bonding-pads.

equally distributed power over all frequency components of the measurement. The first prototype of the UHF-120 was used in our experiments. A special signal excitation is employed to avoid leakage effects in the vibration-frequency spectrum derived by software in the interferometric system. Thus, it is now possible with the utilization of SMBV100A signal generator to obtain the uncertainties discussed in [7] up to 1.2 GHz. Measurements up to 1.2 GHz are demonstrated for the first time by employing a novel bandwidth expansion algorithm [6].

II. PZT TRANSDUCED CONTOUR-MODE RESONATORS

PZT (lead zirconate titanate) is a favorable material to facilitate an electromechanical transduction because it has a large electromechanical coupling coefficient ($k_t{}^2$ = 35% in thickness-extensional mode) [8]. The resonance frequency of vibration for contour mode resonators is defined by lithography. Therefore, contour-mode filters are preferred for realizing multi-band and multi-frequency filters on a single-chip [9].

A. High-overtone Width-extensional Mode Resonator

The bulk-extensional mode resonance of a width-extensional mode (WEM) resonator depends on W, with frequency of operation f given by:

$$f = \frac{n}{2W}\sqrt{\frac{E}{\rho}} \tag{1}$$

where W is the width of the resonator, E and ρ are effective elastic modulus for 2D expansion and density of the resonator respectively, and n is the harmonic order. Higher frequency overtone modes of the WEM resonators are selectively excited by patterning electrodes in differential interdigitated configuration on top of the resonator as shown in Figure 1 (a) [10]. ANSYS modal analysis of the resonator is demonstrated in Figure 1 (b).

B. Fabrication Process

The device fabrication is largely based on the fabrication sequence outlined in [11] with additional improvements in the process to eliminate the pad capacitances. PZT is well known to have a large permittivity that can lead into large pad capacitances. Therefore, in this refined fabrication process, the air-bridge metal routings were implemented to carry electrical signals while avoiding large capacitances from the bond-pads. Due to poor crystallinity and repeatability of the piezoelectric thin-films we have chosen to use the piezoelectric material for actuation and sensing, while utilizing single-crystal silicon as the resonating structure. The SEM image of a PZT transduced high-overtone WEM resonator on single-crystal silicon is presented in Figure 2. In this effort, PZT transduced resonators were fabricated with a 10 μm thick silicon device layer.

C. Electrical Characterization

The resonator was characterized electrically on a Cascade RF probe station after performing a standard SOLT calibration. The DC bias is superimposed to the AC signal at both input and output ports using bias-T's for all measurements. The transmission response of the resonator in air at room temperature and pressure is shown in Figure 3.

III. HETERODYNE LASER-DOPPLER INTERFEROMETRY

A. Ultra High Frequency Heterodyne Vibrometer

The heterodyne interferometric system similar to [7] was used to characterize the high-overtone WEM resonator. A significant improvement in signal excitation has been developed to open possibility to apply high-power, broad-band stimulus signals with equally distributed power over all frequency

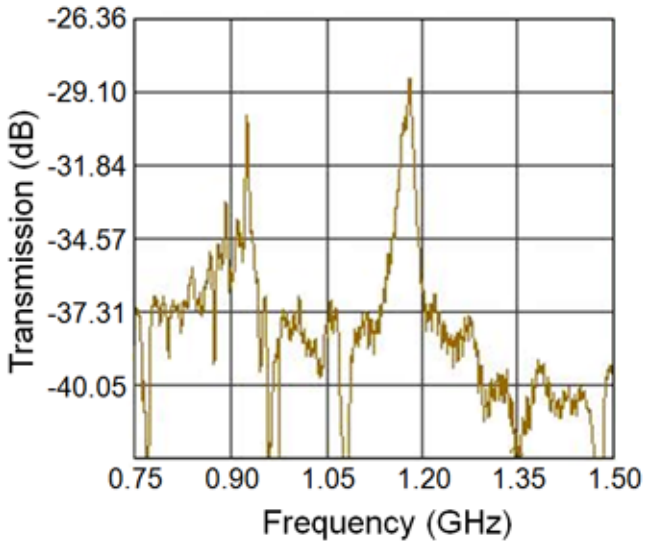

Fig. 3. Measured transmission of a PZT transduced high-overtone width-extensional resonator on 10 μm silicon in air at room temperature and pressure.

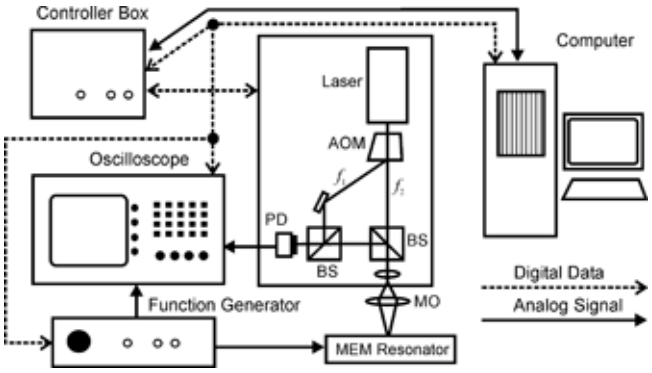

Fig. 4. Schematic of the interferometer system. BS is the beam splitter, PD is the photo detector, MO is the microscope objective, and AOM is the acousto-optical modulator (Bragg-cell).

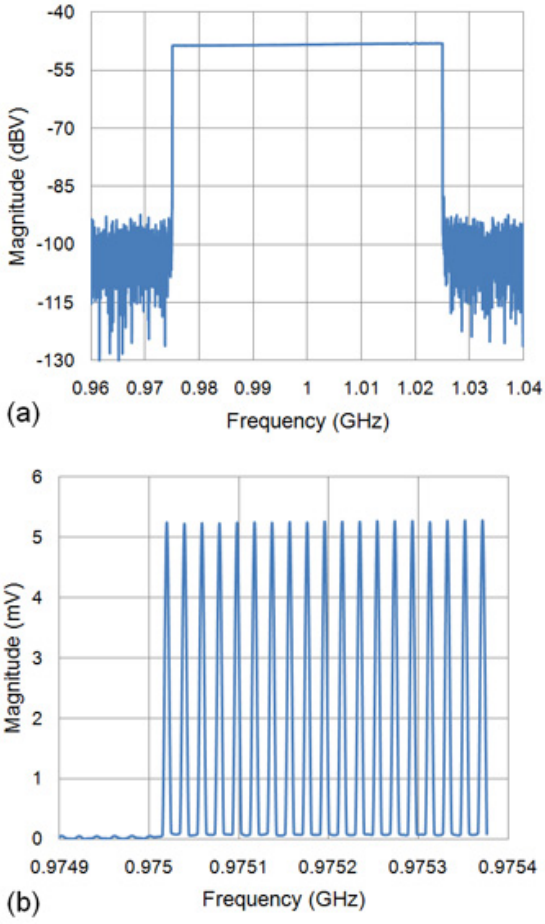

Fig. 5. (a)Spectrum of the broad-bandwidth excitation signal shows a uniform distribution of the energy over the frequency components. (b) Measurement of the periodic-chirp excitation signal with the spectrum resolution four times higher than the distances between the frequency components in the periodic chirp to make the single frequency components of the excitation signal visible in the spectrum.

components in the measurement. A Bragg-cell in our Mach-Zehnder interferometer causes a frequency shift of 613 MHz between reference and measurement beam. A photo detector with a flat amplitude-transfer characteristic detects a heterodyne carrier signal which is phase-modulated by the vibrations of the resonator. The detected RF signal is sampled with a high-frequency digital oscilloscope as shown in Figure 4. The detected signal is transferred to a computer through a LAN connection. The demodulation of the phase-modulated carrier is performed numerically in the computer by software. This software (for our experiments we used the unreleased first beta version of the Polytec Vibsoft with support for the UHF-120) also obtained the data from the oscilloscope and demodulated the carrier signal by means of the arctan-method to compute the vibration spectra [6]. A high laser power of 5 mW in the measurement and reference beam is necessary to obtain a measured noise level in the detector signal which corresponds to less than 3 fm/$\sqrt{Hz}$ (for vibration frequencies $>$ 1 MHz) for a demodulated signal obtained from an ideal noise-free decoder. The resonators were excited with a broad-bandwidth excitation signal generated by the Rohde & Schwarz vector-signal generator SMBV100A that can provide excitation signals with a bandwidth of 120 MHz up to 3.2 GHz and can be programmed with arbitrary waveforms.

B. Signal Excitation with SMBV100A

The SMBV100A is equipped with the options SMBV-B103 (frequency range 9 kHz-3.2 GHz), SMBV-B10 (base-band generator for arbitrary waveforms) to enable the generation of periodic-chirp signals. In this configuration the generator can compute a digital baseband I/Q signal, which is analog converted to modulate the RF carrier of the generator. This enables the generator to provide periodic-chirp signals with 120 MHz bandwidth over the full 1.2 GHz measurement range of the UHF-120. For our experiments we have used the "Multicarrier Continuous Wave" function of the generator (option SMBV-K61), that can generate a number of carriers, equally spaced with an adjustable frequency separation.

The best result with respect to uniformity of the excitation-energy distribution of the exited fast Fourier transform (FFT) bins of the measured vibration spectra was achieved when the following three conditions are met:

1. The distance of the frequency components of the periodic-chirp (carrier spacing) is separated by the same amount as the resolution bandwidth (RBW) of the measurement (the width of one FFT bin).
2. The frequency of the carrier has to be an integer multiple of the RBW (the distance between frequency components).
3. The number of components of the periodic-chirp signals has to be odd to equalize the number of components on the left and right side of the carrier frequency.

This procedure ensures that one period of the excitation signal matches exactly the data acquisition time which is necessary to avoid the leakage in the FFT computation of the vibration spectrum. The excitation signal is split by a power divider and the signal is also sampled simultaneously with another channel of the digital oscilloscope. This gives a feedback of the signal quality and enables us to perform complex averaging of the spectrum. Figure 5 (a) shows a measured spectrum of the excitation signal. In Figure 5 (b), we set the resolution of the spectrum four times higher than the distances between frequency components in the periodic-chirp signals to make the single frequency components of the excitation signal visible in the spectrum. It is demonstrated that leakage effects are negligible and that the strength of the signals is uniformly distributed over all frequency components.

C. Gate Function for the Laser Power

The UHF-120 has a gate to switch the laser power between low (50 μW) and high (5 mW). This feature is important to avoid over saturation of the integrated camera during adjustment of the resonator under test and to minimize the energy transfer from the laser beam to the sample. A power area density of 5 GW/m^2 is generated when the 5 mW laser beam is focused on a spot with an area of 1 μm^2. Thus, the laser beam may have an influence to small and sensitive structures. For example, it may heat-up the sample and shift the resonance frequency of a high-Q MEMS resonator. Therefore, it is a necessary to impinge the full laser power only during data acquisition. In order to quantify this heating effect, a typical case of measurement can be considered. The total energy generated by the laser beam within 10 μs is 50 nJ. Silicon has a reflectivity of roughly 30% and an absorption coefficient of roughly 1 μm^{-1}. Thus, a single-crystal silicon with dimensions of 1 μm^3 absorbs a heat Q of approximately 35 nJ during 10 μs. Such a silicon cube weights approximately 2.33 ng and has a specific heat capacity c of 703 J/(kg.°K). The maximum possible heat up by the laser pulse would be $\Delta T = Q/(c.M) = 21$°C. The heat loss during this period of time would limit the increase of temperature further. However, this method has to be applied for sensitive samples.

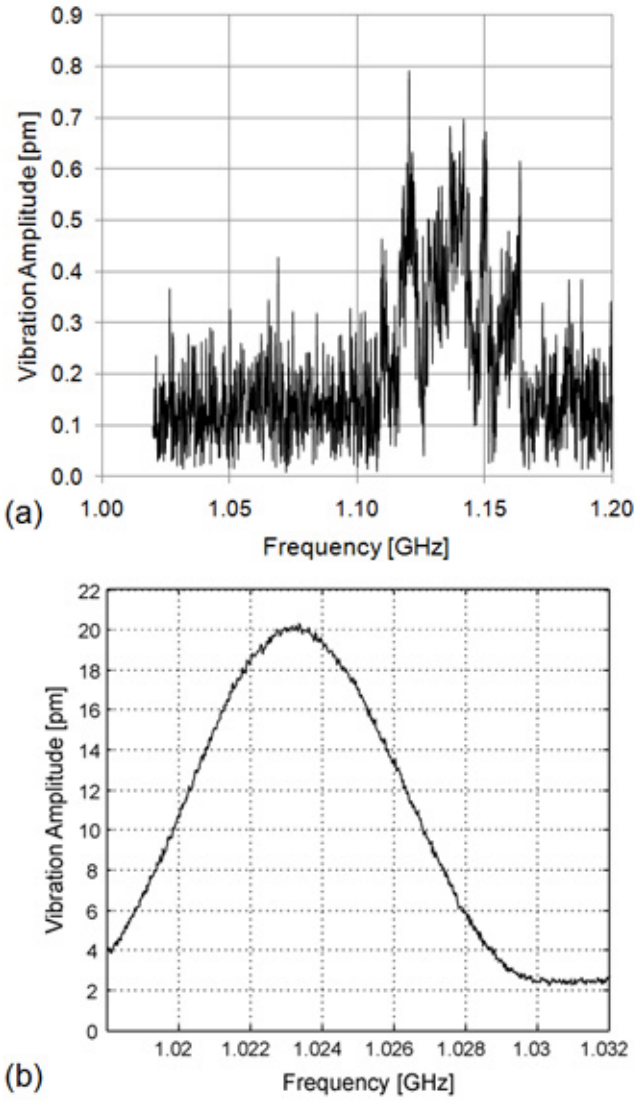

Fig. 6. Optically measured single point displacement of the high-overtone WEM resonator as a function of frequency by the heterodyne laser-Doppler vibrometer (a) RBW = 156.25 kHz and (b) RBW = 19.53125 kHz.

The SMBV100A offers a convenient method to generate the gate function for the heterodyne interferometer which is also used to trigger the measurement. The generator features a so called marker output that can be set to a high or low state (TTL) for a certain period by defining a number of time increments. These time increments correspond to the samples of the digital baseband generator. It is necessary that the high period of the gate signal corresponds to the data acquisition time during which the vibrating specimen is impinged by the full laser power. The total number of samples of the gate signal (high-level + low-level) has to be a multiple of the sample number of the signal period. This condition is important to ensure a constant phase of the generator signal with respect to the measurement. A careful attention to these measurement conditions ensures the uniform signal excitation which will prevent leakage effects in the digital measurement data.

D. Optical Characterization of a high-overtone WEM resonator

By using this heterodyne laser-Doppler vibrometer system we characterized our high-overtone WEM resonator. The single point optical measurement was performed in air at room temperature and pressure. RF power of +10 dBm was applied to electrically drive the resonator. The measurement was taken using a sampling rate of 40 GS/s at the digital oscilloscope. We measured the mechanical displacement of the resonator at resonance frequency of 1.15 GHz as shown in Figure 6 (a). The measurement uses a 156.25 kHz RBW, thus a relatively high noise level is observed in Figure 6 (a). However, our measurement system and configuration can suppress the displacement noise level below 0.3 pm even with a relatively large RBW. The displacement noise around the vicinity of the resonance peak was caused by a problem with synchronization of the excitation signal, as we were using complex averaging. From our observation, at frequency above 1 GHz, even a minor phase jitter can cause problems and distort the measurement results. A smaller RBW was used to measure the subsequent resonator in the same wafer. As the result of using 19.53125 kHz RBW, we were able to acquire data with much better noise level as shown in Figure 6 (b).

IV. Effect of Anchor Design in a WEM Resonator

A proper suspensions design is very crucial for RF MEMS resonators, because the anchors of MEMS resonators can be designed to attenuate or amplify certain modes of vibrations. Using the same mask set as the previously discussed high-overtone width-extensional mode resonator, we also fabricated the width-extensional mode resonator as shown in Figure 7. An array of PZT transduced width-extensional mode resonators with different anchor lengths was designed and fabricated. We electrically measured the frequency response of PZT transduced width-extensional mode resonators with various anchor lengths.

From our experimental results, we found certain anchor lengths that suppress the desired mode of vibration and gives a rich frequency response as shown in Figure 8. Electrical measurement has a limited ability to identify the mode shape corresponding to each resonance peak in this rich frequency response. Additional complications introduced by uncertain fabrication errors cause the mode shape of vibration becomes even more difficult to identify. By using the heterodyne laser-Doppler interferometric measurement technique that was presented earlier, we were able to do the 2D scanning in X-Y plane and reconstruct the 3D mode of vibration for each resonance peak of the rich frequency response as shown in Figure 9. By observing these 3D modes of vibrations in Figure 9, we can conclude that these particular anchor dimensions are favorable to excite the high harmonics of flexural modes and thickness modes. We can also see that the vibration amplitudes of these modes are less than 100 pm, which is smaller by a factor of 5 compared to the mechanical displacement of the desired mode of vibration at resonance.

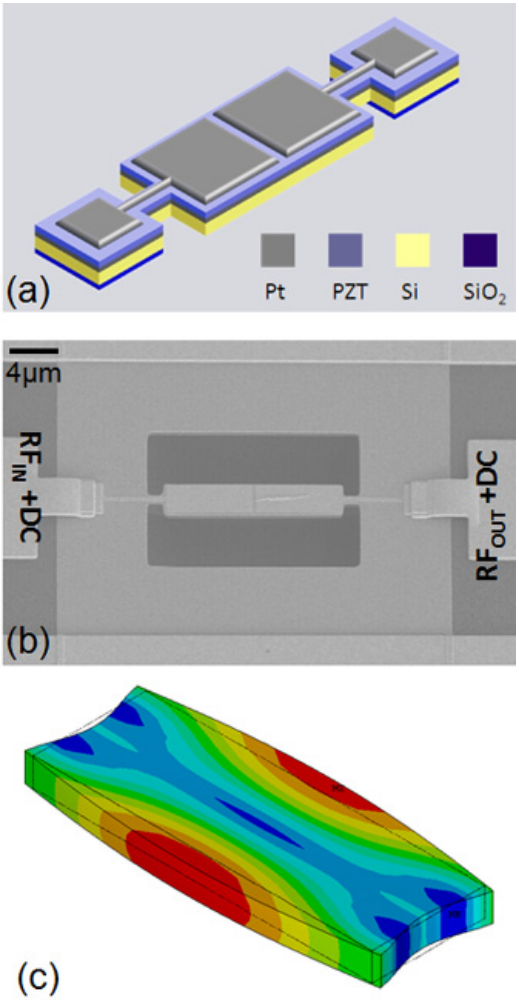

Fig. 7. (a) Schematic, (b) SEM image, and (c) ANSYS modal analysis of a width-extensional mode resonator.

These results are very useful for MEMS designers to optimize their resonator design.

V. Conclusion

In conclusion, we have designed and fabricated PZT transduced high-overtone width-extensional mode resonators. The resonator has been characterized electrically and optically with resonance frequency above 1 GHz. An ultra high frequency, broad-band, and non-contact measurement technique for RF MEMS resonators by a heterodyne laser-Doppler interferometric method has been presented. The heterodyne LDV measurement technique has enabled vacuum-compatible characterization method for RF MEMS devices with high accuracy. Thus, various RF MEMS devices that have high sensitivity to air-damping can be characterized using this system while operating inside the vacuum chamber. The heterodyne LDV measurement method was able to identify 3D modes of vibrations of RF MEMS resonators. The 3D mode imaging can provide constructive feedback to RF MEMS designers to optimize their designs.

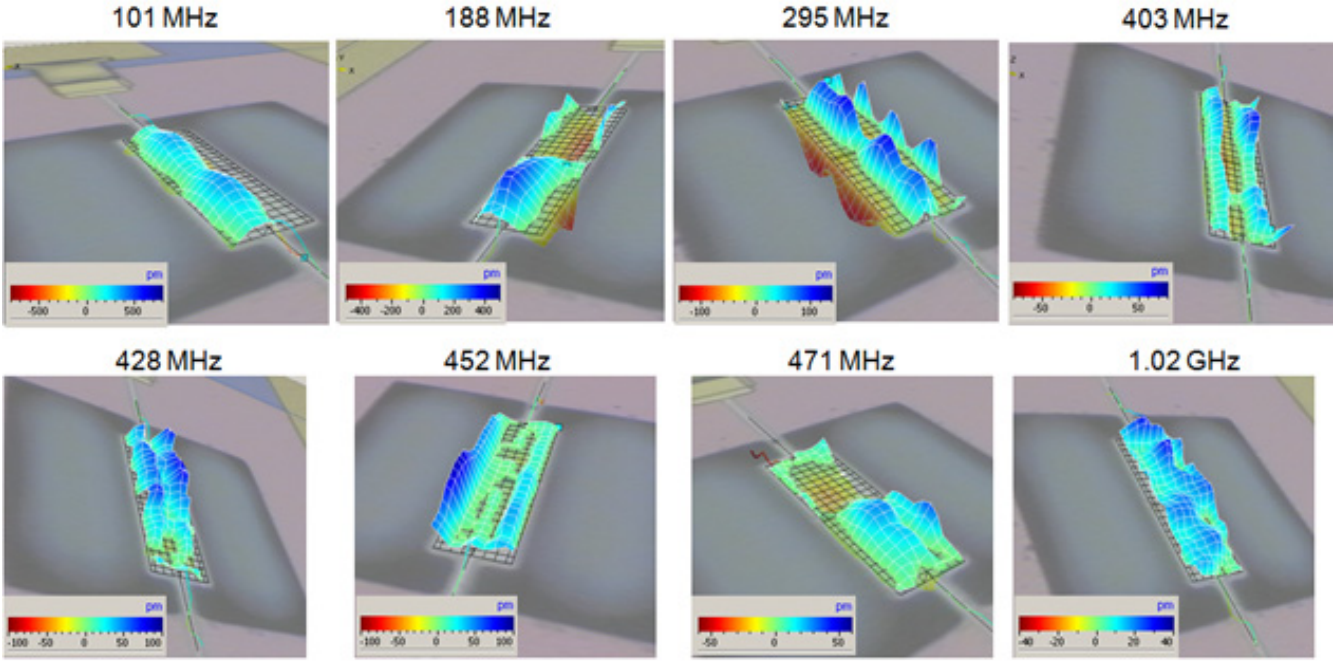

Fig. 9. 3D images of the rich frequency response of a width-extensional mode resonator with improper anchor design.

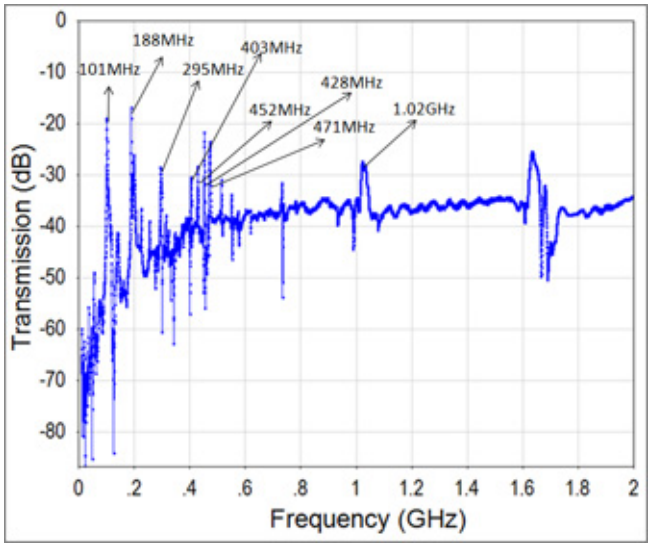

Fig. 8. Rich frequency response of a width-extensional mode resonator with improper anchor design.

ACKNOWLEDGMENT

The authors would like to thank Brian Power, Joel Martin and Richard Piekarz of the Army Research Laboratory for their assistance in fabricating the resonators.

REFERENCES

[1] J. S. Pulskamp, D. C. Judy, R. G. Polcawich, R. Kaul, H. Chandrahalim, and S. A. Bhave, "Monolithically integrated piezomems SP2T switch and contour-mode filters," *Proceedings of the IEEE International Conference on Micro Electro Mechanical Systems (MEMS)* , pp. 900 – 903, 2009.

[2] A. San Paulo, E. Quevy, J. Black, R. T. Howe, R. White, and J. Bokor, "Mode shape imaging of out-of-plane and in-plane vibrating RF micromechanical resonators by atomic force microscopy," *Microelectronic Engineering* **84**(5-8), pp. 1354 – 1357, 2007.

[3] C. Rembe and R. S. Muller, "Measurement system for full three-dimensional motion characterization of MEMS," *Journal of Microelectromechanical Systems* **11**(5), pp. 479 – 488, 2002.

[4] J. D. Larson III, R. C. Ruby, and K. L. Telschow, "Observation of flexural modes in FBAR resonators at MHz frequencies," *Proceedings of the IEEE Ultrasonics Symposium* **1**, pp. 88 – 91, (Honolulu, HI, USA), 2003.

[5] J. V. Knuuttila, P. T. Tikka, and M. M. Salomaa, "Scanning Michelson interferometer for imaging surface acoustic wave fields," *Optics Letters* **25**(9), pp. 613 – 615, 2000.

[6] C. Rembe, S. Boedecker, A. Drabenstedt, F. Pudewills, and G. Siegmund, "Heterodyne laser-Doppler vibrometer with a slow-shear-mode Bragg cell for vibration measurements up to 1.2 GHz," *Proceedings of SPIE - The International Society for Optical Engineering* **7098**, (Ancona, Italy), 2008.

[7] S. Stoffels, S. Boedecker, R. Puers, I. De Wolf, H. A. C. Tilmans, and C. Rembe, "Measuring the mechanical resonance frequency and quality factor of MEM resonators with well-defined uncertainties using optical interferometric techniques," *Digest of Technical Papers - International Conference on Solid State Sensors and Actuators and Microsystems, TRANSDUCERS '09* , pp. 549 – 552, (Denver, CO, USA), 2009.

[8] J. D. Larson III, S. R. Gilbert, and B. Xu, "PZT Material properties at UHF and microwave frequencies derived from FBAR measurements," *Proceedings - IEEE Ultrasonics Symposium* **1**, pp. 173 – 177, (Montreal, Que., Canada), 2004.

[9] G. Piazza, P. J. Stephanou, and A. P. Pisano, "Single-chip multiple-frequency AlN MEMS filters based on contour-mode piezoelectric resonators," *Journal of Microelectromechanical Systems* **16**(2), pp. 319 – 328, 2007.

[10] H. Chandrahalim, S. A. Bhave, R. G. Polcawich, J. S. Pulskamp, and D. Judy, "Fully-differential mechanically-coupled PZT-on-silicon filters," *Proceedings - IEEE Ultrasonics Symposium* , pp. 713 – 716, 2008.

[11] H. Chandrahalim, S. A. Bhave, R. Polcawich, J. Pulskamp, D. Judy, R. Kaul, and M. Dubey, "Performance comparison of $Pb(Zr_{0.52}Ti_{0.48})O_3$-only and $Pb(Zr_{0.52}Ti_{0.48})O_3$-on-silicon resonators," *Applied Physics Letters* **93**(23), p. 233504, 2008.